SAND2017-9420C

Modeling for Metal Additive Manufacturing

MJ Martinez and DR Noble
Engineering Science Center
Sandia National Laboratories

Contributors: D. Bolintineanu, K. Johnson, K. Ford, J. Bishop, T. Rodgers

USACM-TMS Additive Manufacturing Conference/Workshop

Sept. 8, 2017

SAND2017-XXXX

Modeling Workflow for Additive Manufacturing

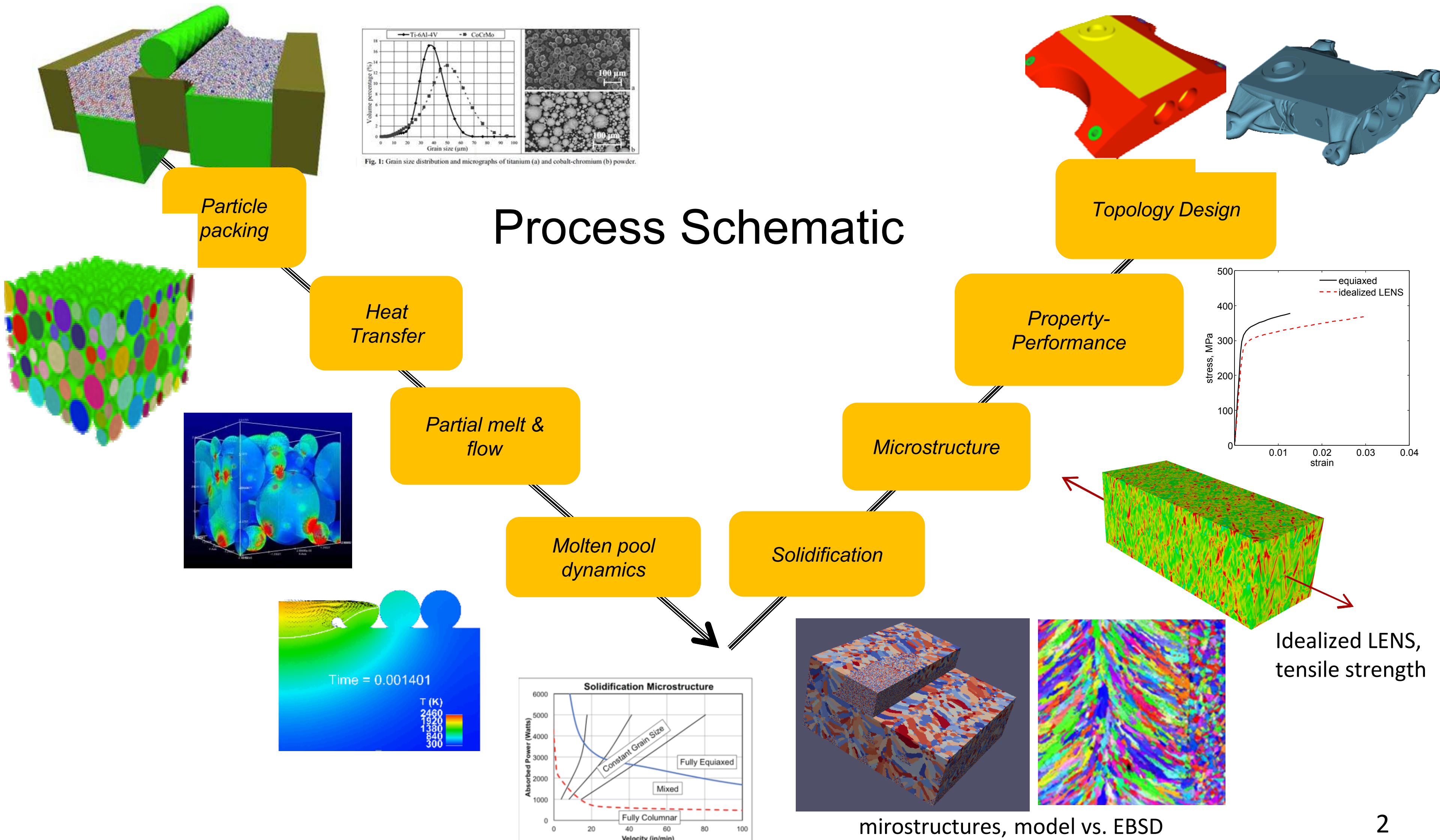

SNL Modeling Capabilities

Codes
LAMMPS, SPPARKS,
Sierra/Aria,
Sierra/Adagio

Part Scale Thermal & Solid Mechanics
Kyle Johnson, Kurtis Ford & Joe Bishop

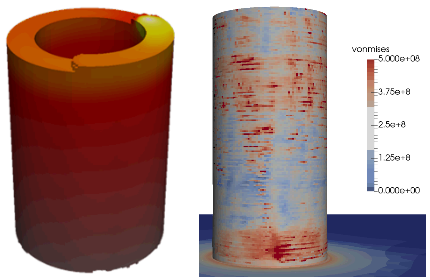

Mesoscale Selective Laser Melting
Mario Martinez & Brad Trembacki

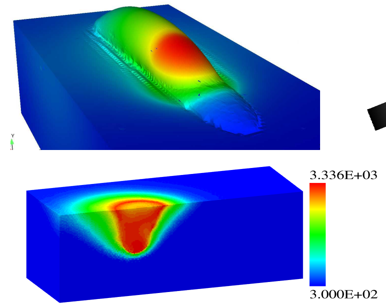

Powder Spreading
Dan Bolintineanu

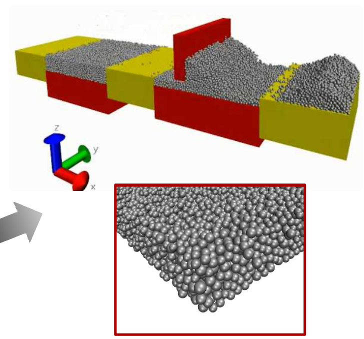

Powder Behavior
Mark Wilson

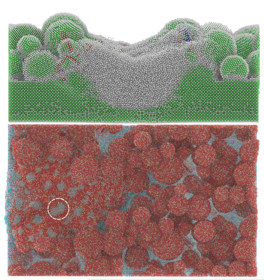

Part Scale Microstructure
Theron Rodgers

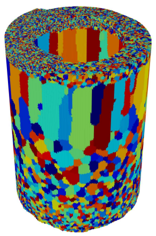

Mesoscale Texture/Solid Mechanics/CX
Judy Brown, Theron Rodgers and Kurtis Ford

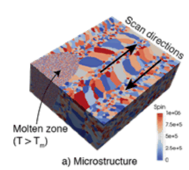

10^{-6} 10^{-3} 1

Length Scale (m)

Powder Dynamics: Background and Motivation

Layer-by-layer powder bed fusion processes (e.g. SLM/SLS):

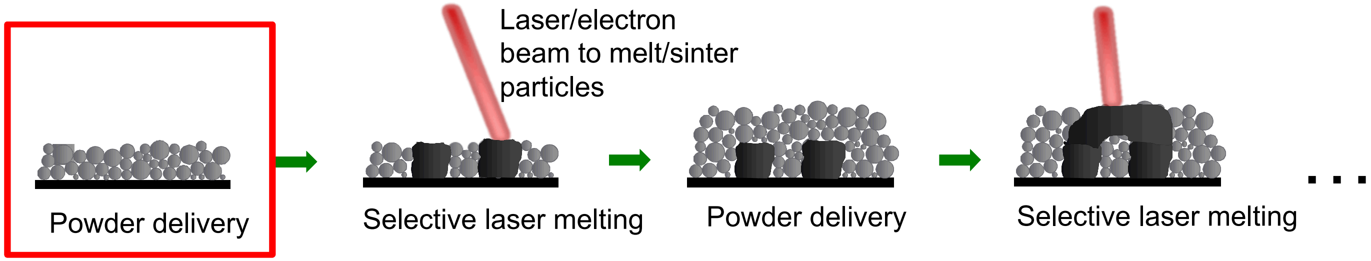

- First step in AM powder bed process
  - Powder bed surface can affect laser interaction; power bed packing can affect void formation, surface finish, thermal properties
  - Informs downstream process models
- Variability in powder properties due to vendor supply, powder recycling
- Several key process length scales are comparable to individual particles:

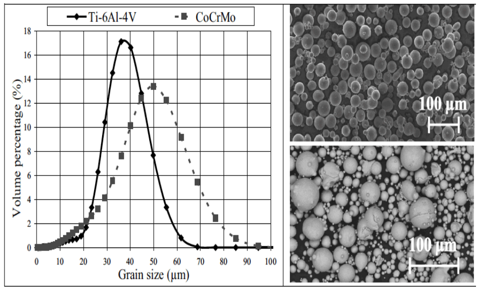

From Ref. 1

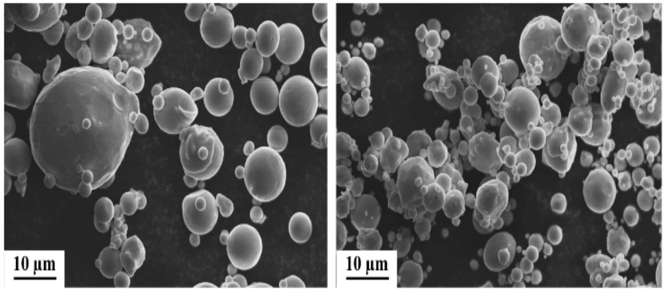

From Ref. 2

Typical particle diameter: 10-100 µm

Powder layer thickness 30-150 µm
Laser beam spot size 70-200 µm (ref. 1)

1. Vandenbroucke, B. and Kruth, J.P. *Rapid Prototyping Journal* 13 (2007): 196
2. Yadroitsev, I., et al. *Journal of Laser Applications* 25 (2013): 052003

D. Bolintineanu, J Lechman, 1516

Modeling powder dynamics using DEM

- **D**iscrete **E**lement **M**odeling: molecular dynamics-like method
  - Each particle modeled explicitly (position, velocity, angular velocity)
  - Forces/torques computed at contact using reduced order models
  - Dynamics integrated in time for large collection of interacting particles

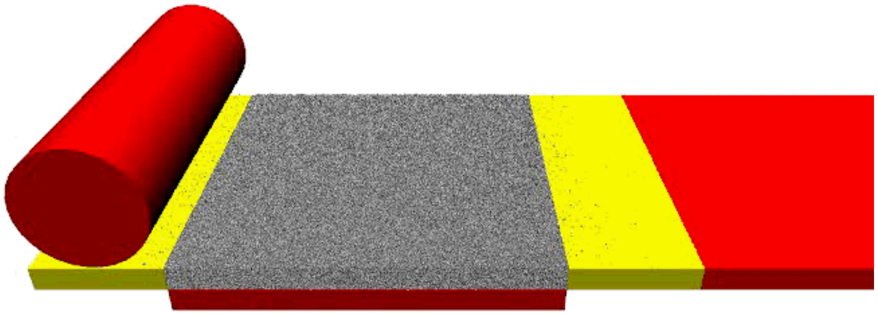

Free, open-source LAMMPS: https://lammps.sandia.gov

Large resulting data:

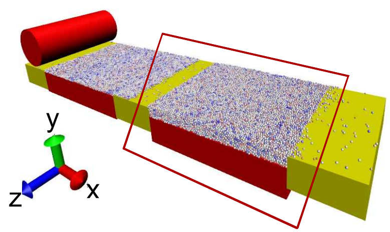

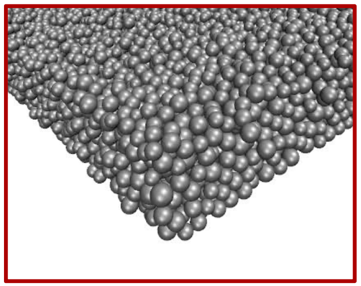

Powder bed surface properties:

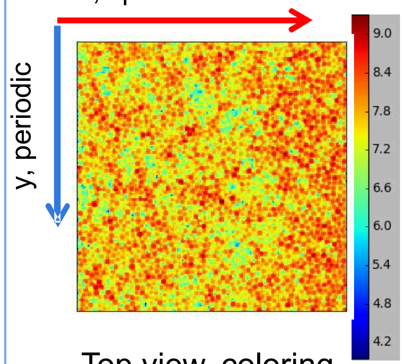

Top view, coloring corresponds to height

S_a: surface roughness

Height profile: height averaged over x

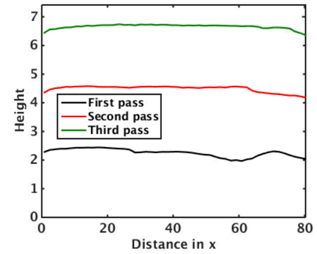

Height autocorrelation function:

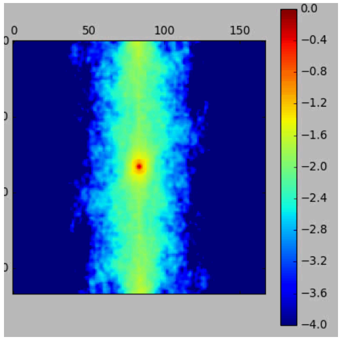

Local particle contact properties

- Coordination number distribution
- Contact size distribution
- Fabric tensor

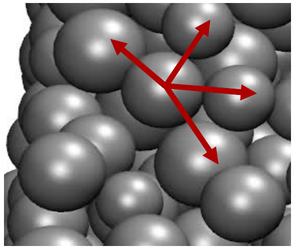

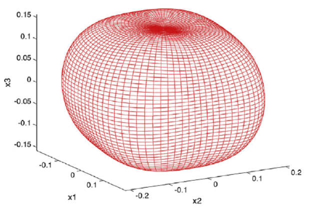

Stershic et al, J Power Sources, v. 297, p540

Powder bed bulk properties:

- Porosity(x), porosity(z)
- Pore size distribution
- Two-point correlation function
- 'Coarseness': variability as a function of length scale
- Lineal path function, chord length distribution

. . .

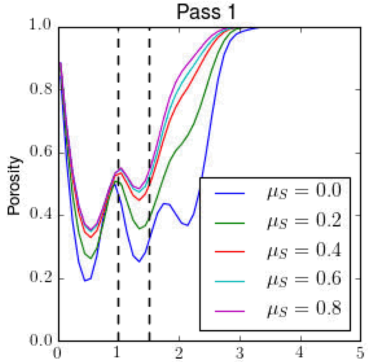

Relevant Sandia Thermal/Fluid Applications to Burn and Melt using Enriched FEM

Numerous problems with moving or topologically complex interfaces with discontinuous physics and fields

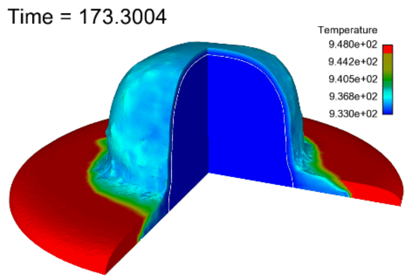

Aluminum Melt

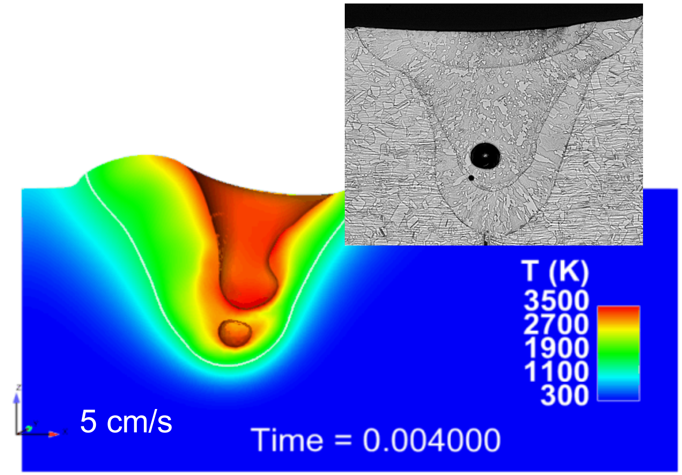

Laser welding

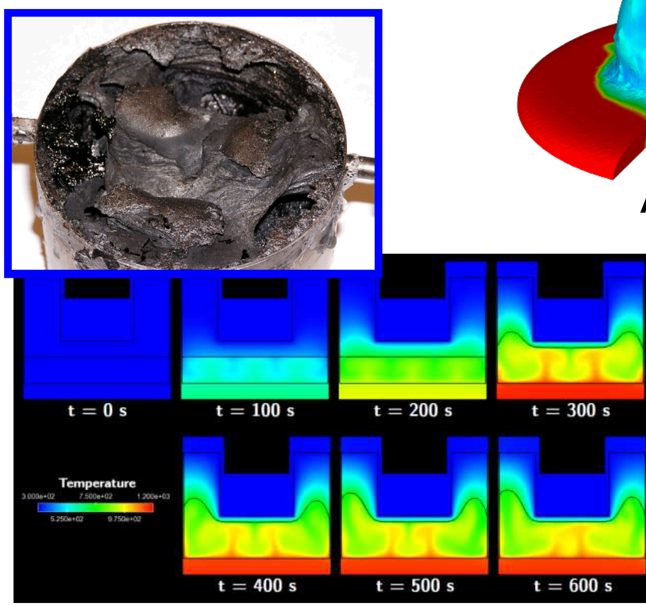

Organic Material Decomposition (OMD) with coupled porous and low Ma flow

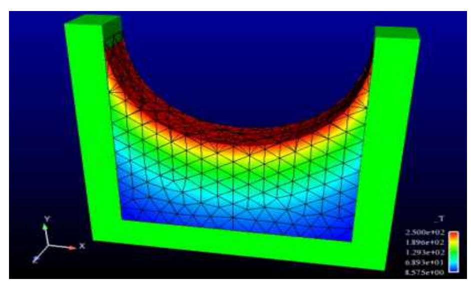

Material death

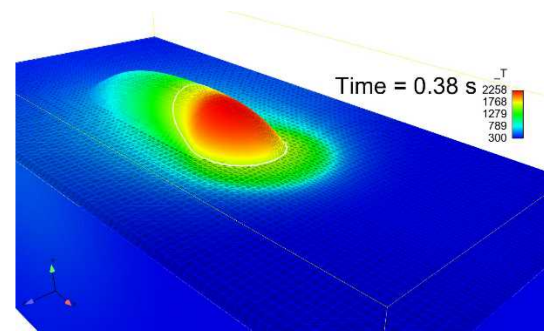

Additive Manufacturing

Conformal Decomposition Finite Element Method (CDFEM)

- Simple Concept (Noble, et al. 2010)
  - Use one or more level set fields to define materials or phases
  - Decompose non-conformal elements into conformal ones
  - Obtain solutions on conformal elements
- Related Work
  - Li et al. (2003) FEM on Cartesian Grid with Added Nodes
  - Ilinca and Hetu (2010) Finite Element Immersed Boundary
  - S. Soghrati and P.H. Geubelle (2012) Interface Enriched Finite Element
- Properties
  - Supports wide variety of interfacial conditions (identical to boundary fitted mesh)
  - Avoids manual generation of boundary fitted mesh
  - Supports general topological evolution (subject to mesh resolution)
- Similar to finite element adaptivity
  - Uses standard finite element assembly including data structures, interpolation, quadrature

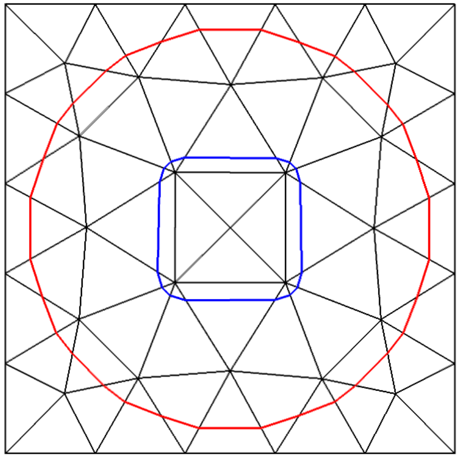

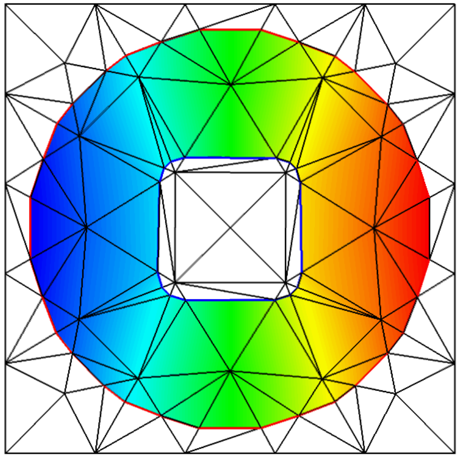

Finite Element Methods for Moving Interfaces in Fluid/Thermal Applications Tested at Sandia

		Enriched Finite Element Methods	
ALE	Diffuse LS	XFEM	CDFEM
• Separate, static blocks for gas and liquid phases • Static discretization 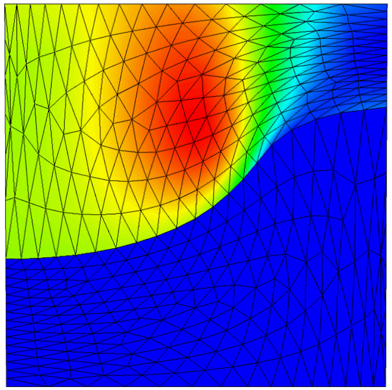	• Single block with smooth transition between gas and liquid phases • Static discretization 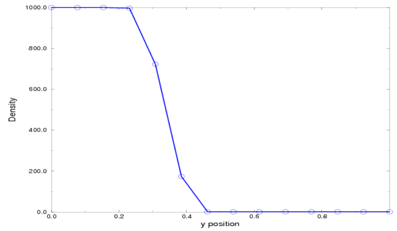 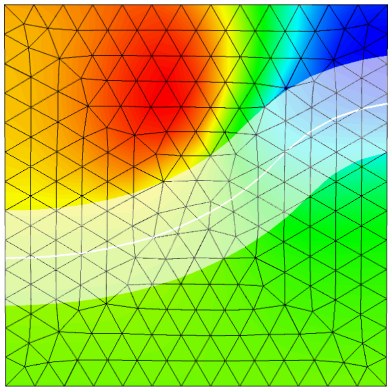	• Single block with sharply enriched elements (weak or strong) spanning gas and liquid phases • Interfacial elements are dynamically enriched to describe phases	• Separate, dynamic blocks for gas and liquid phases • Interfacial elements are dynamically decomposed into elements that conform to phases 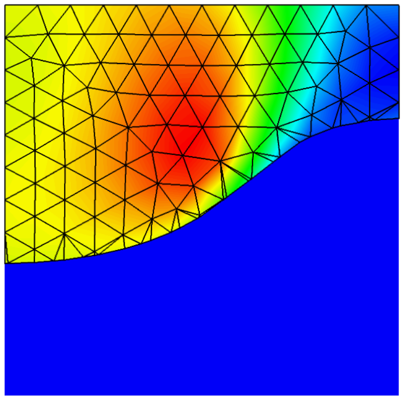

Formulation: Interface Dynamics

- Level Set Equation
  - Advection equation

$$\frac{\partial \phi}{\partial t} + u \cdot \nabla \phi = 0$$

  - Galerkin, Backward Euler

$$\int_{\Omega} \frac{\phi - \phi^n}{\Delta t} N_i \, d\Omega + \int_{\Omega} u \cdot \nabla \phi \, N_i \, d\Omega = 0$$

  - SUPG stabilization

$$N_i \Rightarrow N_i + \tau_\phi \, u \cdot \nabla N_i, \; \tau_\phi = \left[\left(\frac{2}{\Delta t} \right)^2 + u_i g_{ij} u_j \right]^{-\frac{1}{2}}$$

  - Periodic renormalization
    - Compute nearest distance to interface

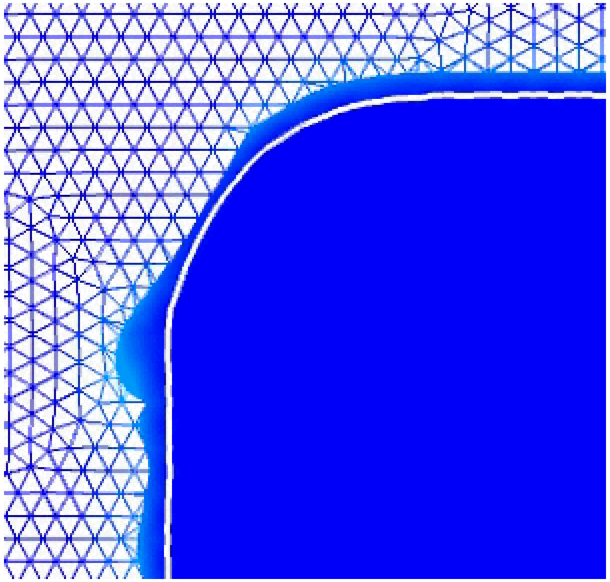

Models: Liquid-Air Interface

- Capillary Force
  - Same model used in ALE simulations
    - Jump in stress due to interfacial tension

$$\int_{\Gamma} \left(\gamma\kappa\,\mathbf{n} + \nabla_s \gamma\right) N_i \; d\Gamma = \int_{\Gamma} \gamma \nabla_s N_i \; d\Gamma, \; \nabla_s \equiv \left(\mathbf{I} - \mathbf{nn}\right)\nabla$$

- Interface Stabilization
  - Surface viscosity type stabilization
    - Based on recent paper by Hysing

$$\int_{\Gamma} \mu_s \nabla_s u \cdot \nabla N_i \; d\Gamma$$

- Radiation
  - Simple radiation boundary condition

$$\int_{\Gamma} \varepsilon\sigma\left(T^4 - T_e^4\right) N_i \; d\Gamma$$

  - Enclosure radiation
    - Enclosure temperature 2000K
    - Repeat viewfactor calculation every time step

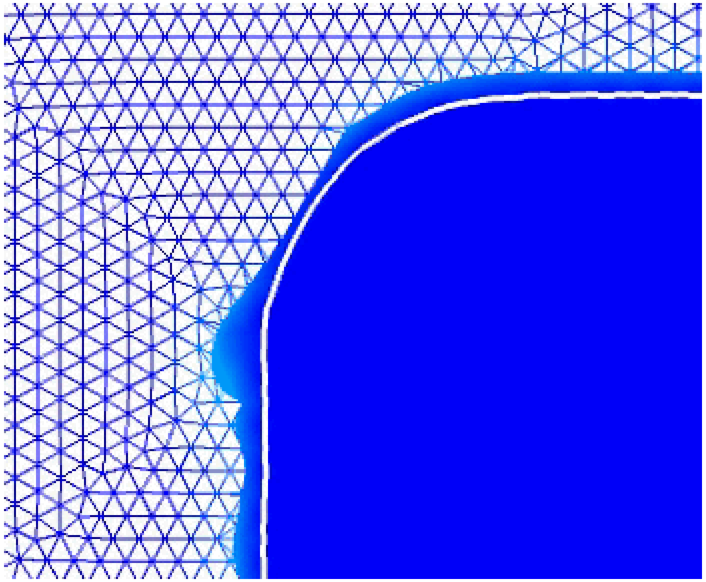

Powder Bed Physics Model

Goal: Link AM mesoscale processes to macroscale performance

Method: Conformal level-set technology includes melt and ambient (or assist) gas dynamics

- Laser energy coupling to particle packs
- Melt/solidification, capillary-driven flow, buoyant gas convection, solutal segregation
- Impact of laser setting: power, spot size, scan rate, hatch spacing, ...
- Laser schedule: edge modulation, variable power, variable spot,
- Beam overlap, remelt, porosity

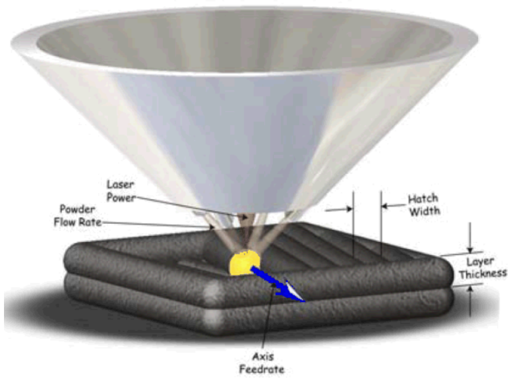

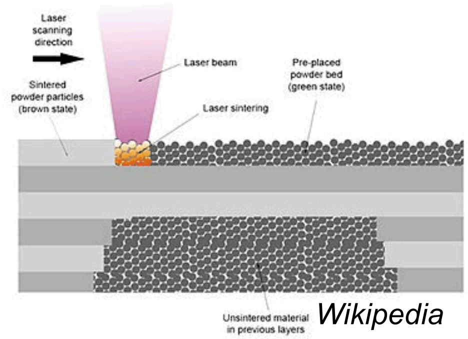

Wikipedia

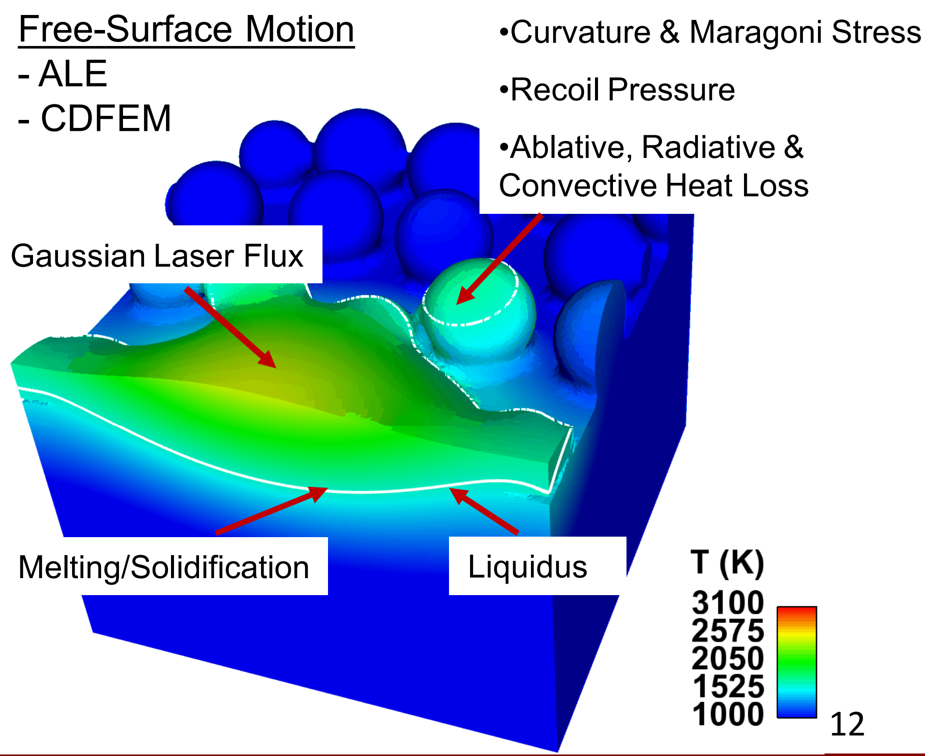

SNL Prox 300 Model

Impact of power for fixed hatch spacing

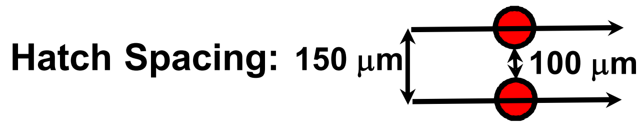

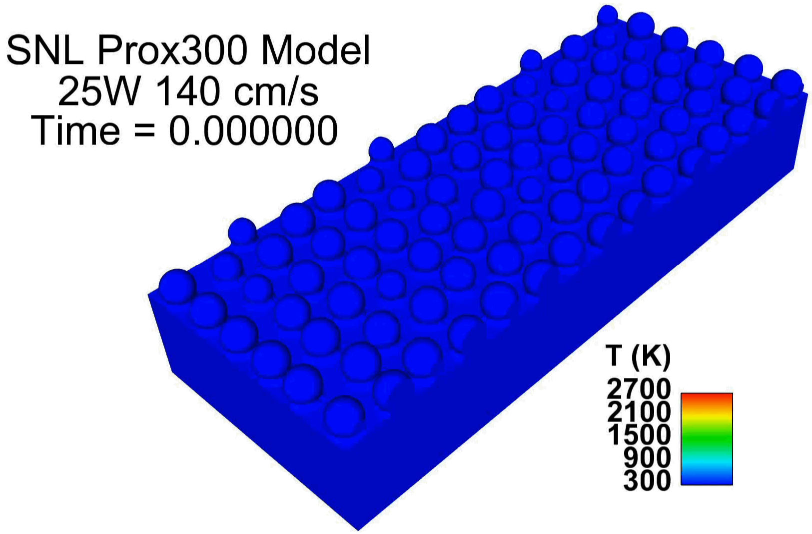

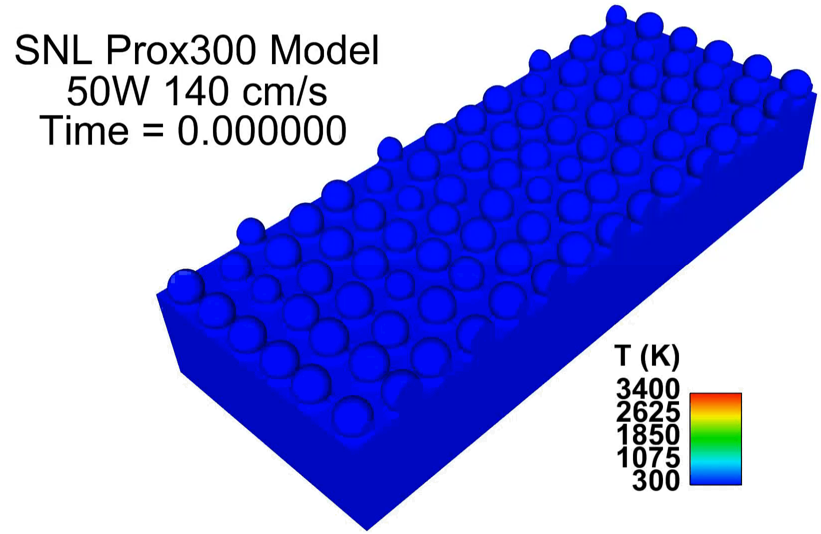

Stainless steel 304L
25 micron powder

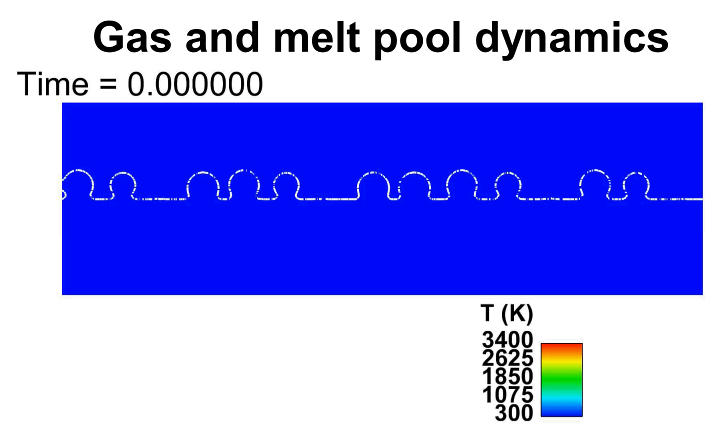

Notes:

- 500 micron powder bed traversed in **357 microsec**.
- Sloshing-driven **gas dynamics** entrains ambient gas

SNL Prox 300 Model
Gaussian Laser 140 cm/s

General features:
- Surface flux melts particles top to bottom;
- Fully molten particles jump into melt pool by capillarity, inciting sloshing

25W
- Shallow melt pool; smaller melt path
- Solidification front freezes in wave peaks and troughs – *ribbed finish*

50W
- Long, deep melt pool; wider melt path
- *Smooth finish* (?)
- Laser power modulated at exit

Power, hatch spacing, and vertical heat penetration can be guided/optimized with melt dynamics models.

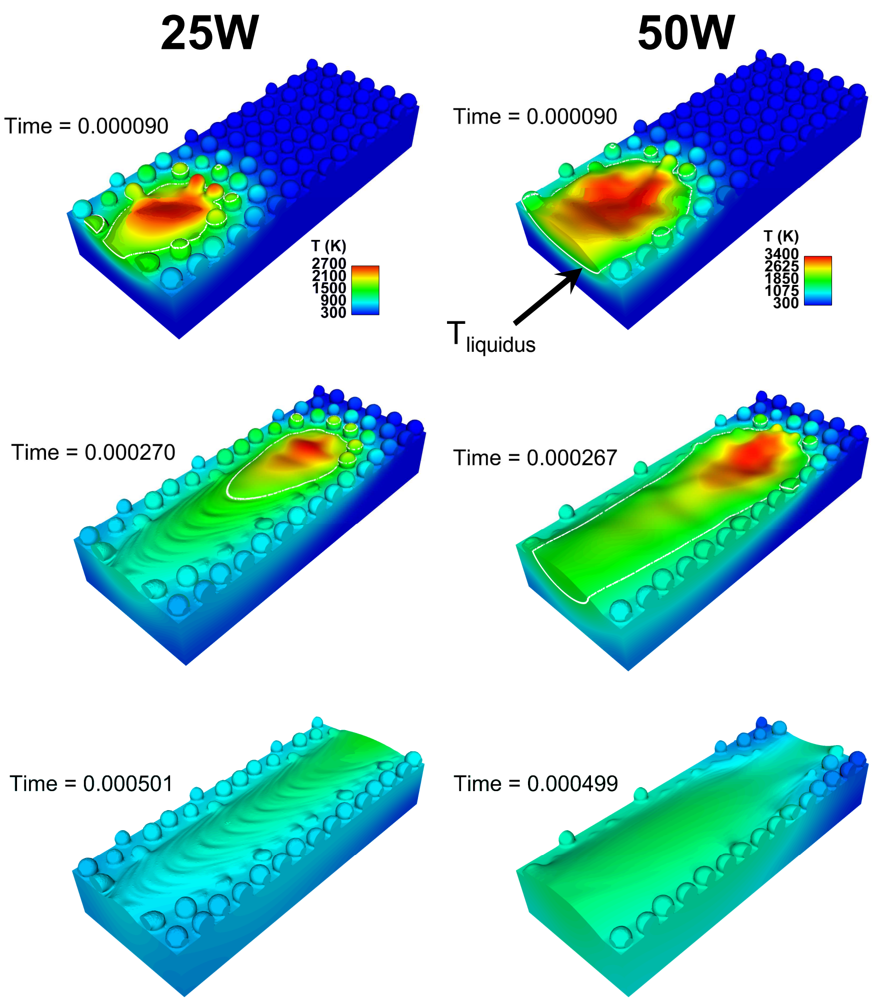

Power and recoil pressure

25W

100 W

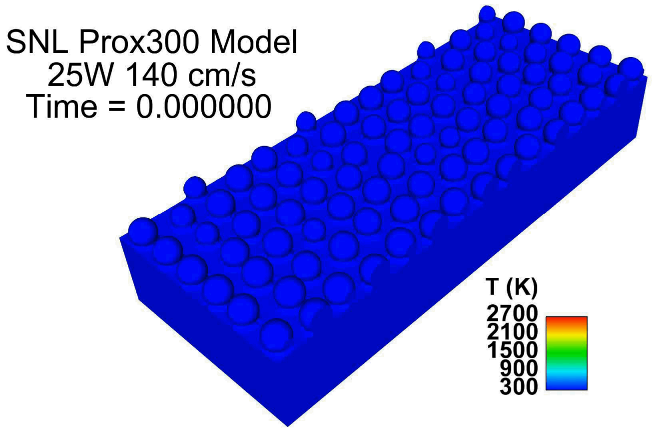

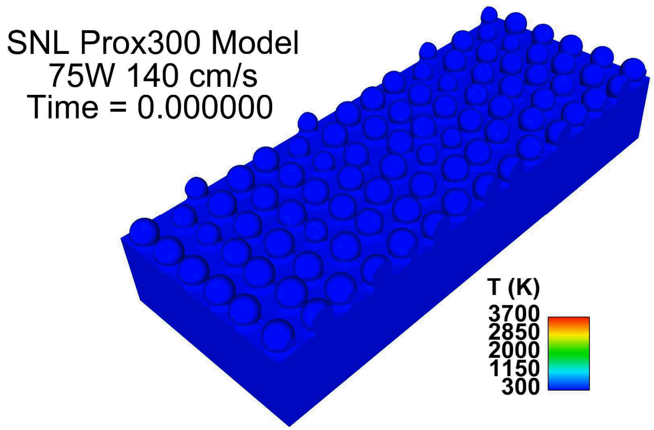

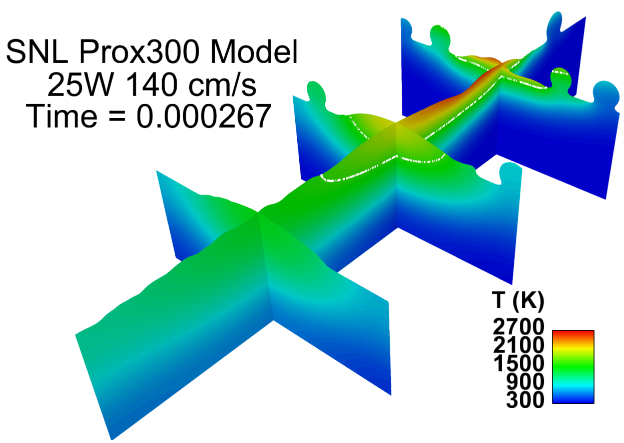

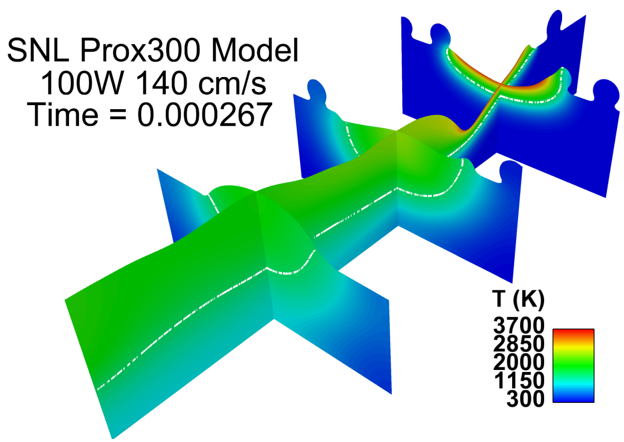

- Small melt pool
- Freezes in surface ripples

- Keyhole (small) at high power
- Recoil pressure → balling effect

Powder porosity

50W Reff=0.6

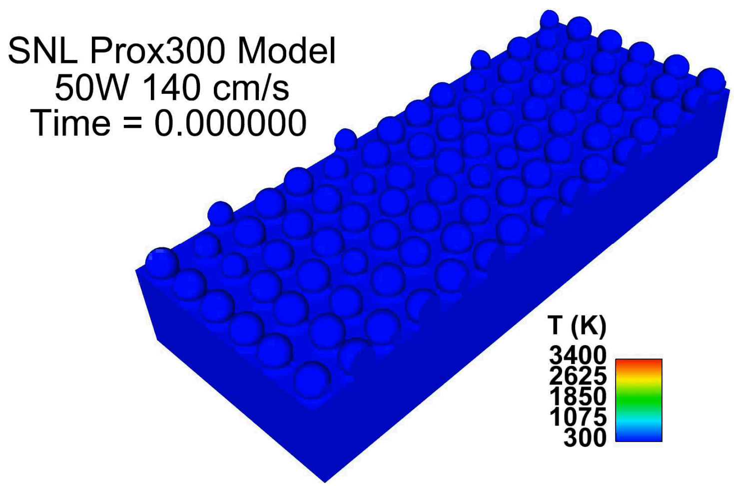

Sparse powder bed
27% solid fraction

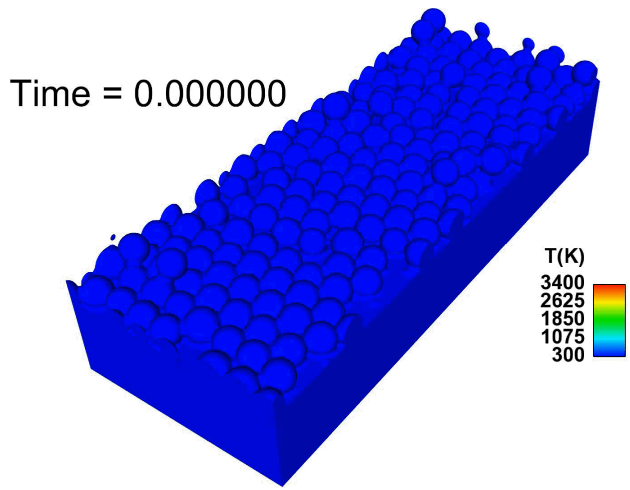

Simulated powder bed
57% solid powder fraction

Lower porosity powder:

- requires more laser power
- Higher void probability

Laser Scan Rate

Energy deposition rate ~ Q/v

50W Reff=0.6

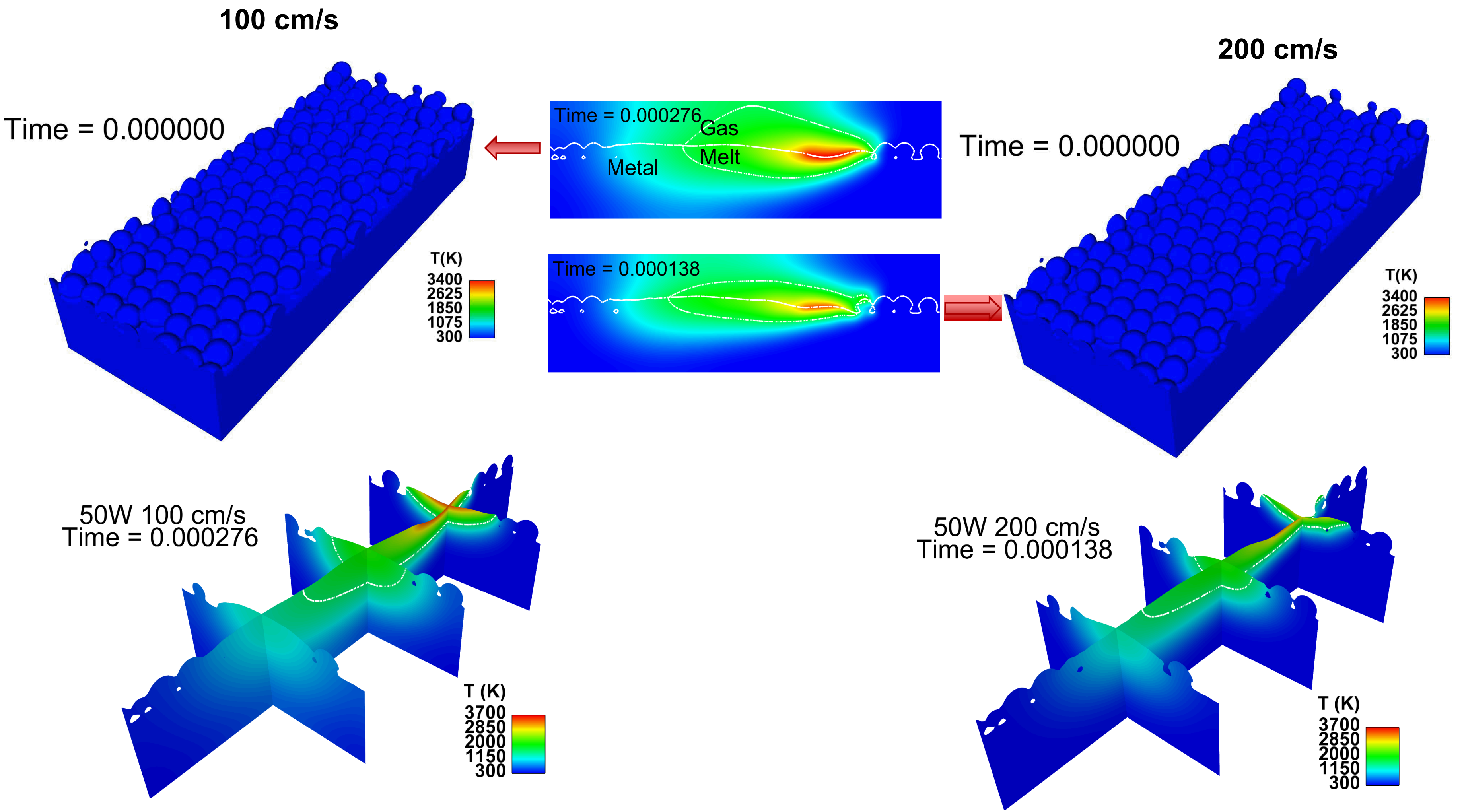

Energy deposition rate and defects

50W CW Laser

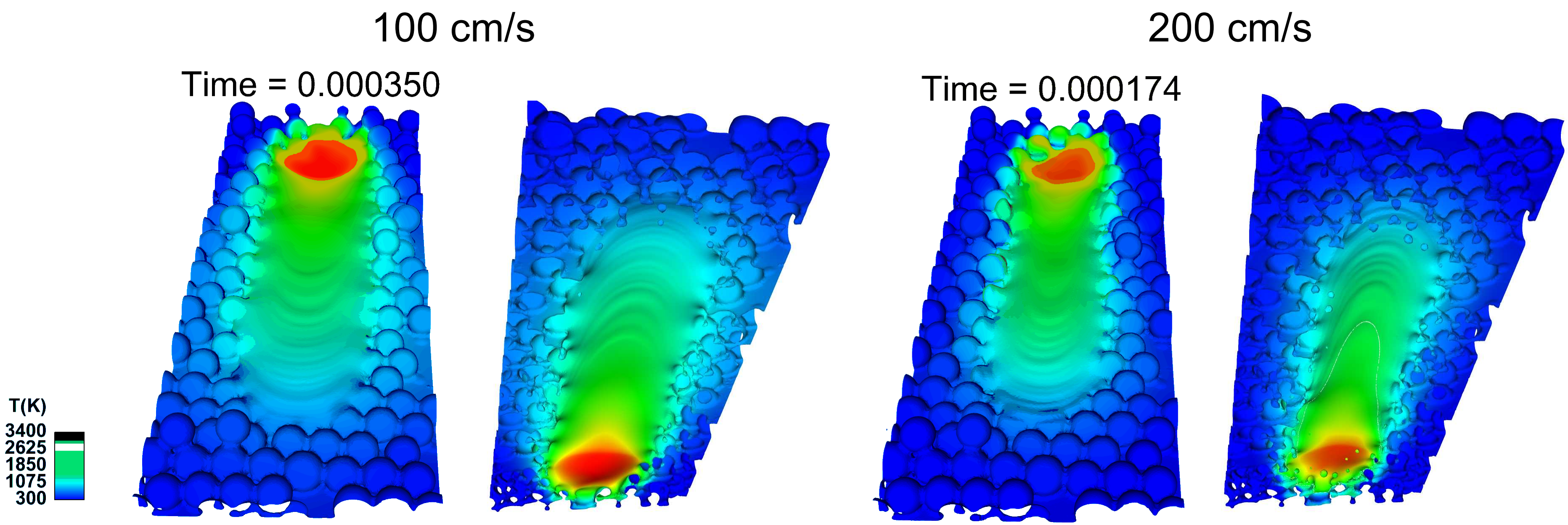

- Energy deposition rate ~ Q/v
- Higher scan rate
  - Lower energy per unit length
  - Narrower track
  - More void left behind

Part-Scale Models:
304L Cylinder Example

Process	Structure	Property	Performance (Future)
Thermal Model in Aria	Microstructure Model in SPPARKS (Theron Rodgers)	Residual Stress in Adagio	Behavior using as-built microstructure, residual stress, and properties

- Cylinder built using LENS process
- Laser diameter = 4 mm
- Laser Speed = 8.46 mm/s
- Layer Thickness = 0.9 mm
- Laser Power = 2000 > 1750 > 1500 > 1250 W

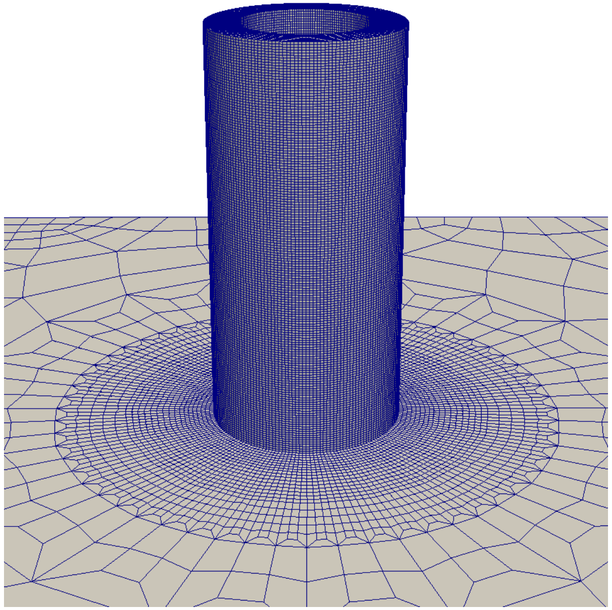

K. Johnson, K. Ford, J. Bishop, 1554

Thermal and Residual Stress Histories

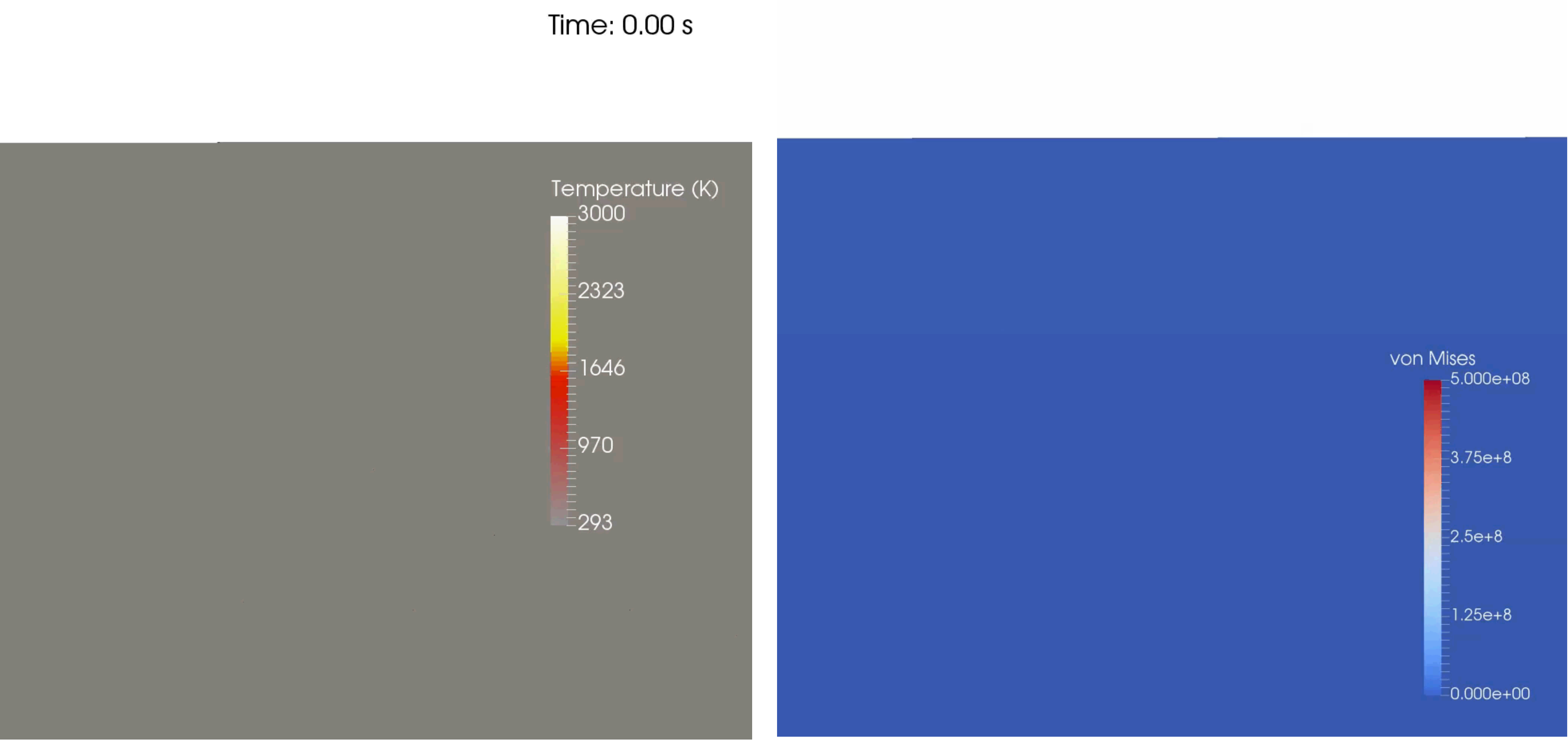

Comparison to IR Imaging

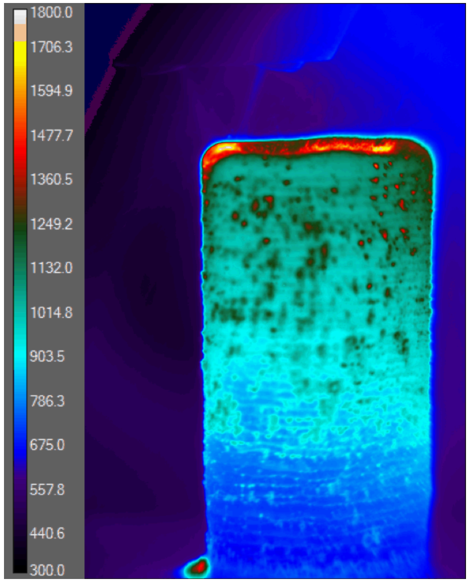

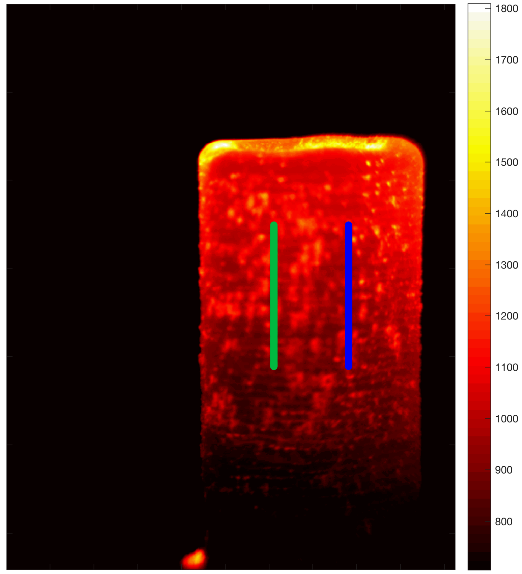

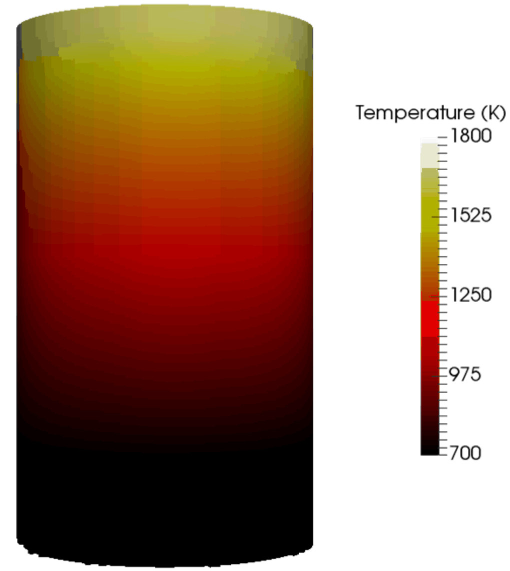

Simulation Results

- IR camera mounted on LENS machine
- Assumes constant emissivity
- Compared to simulation

Final Von Mises and Axial Stress

Sandia National Laboratories

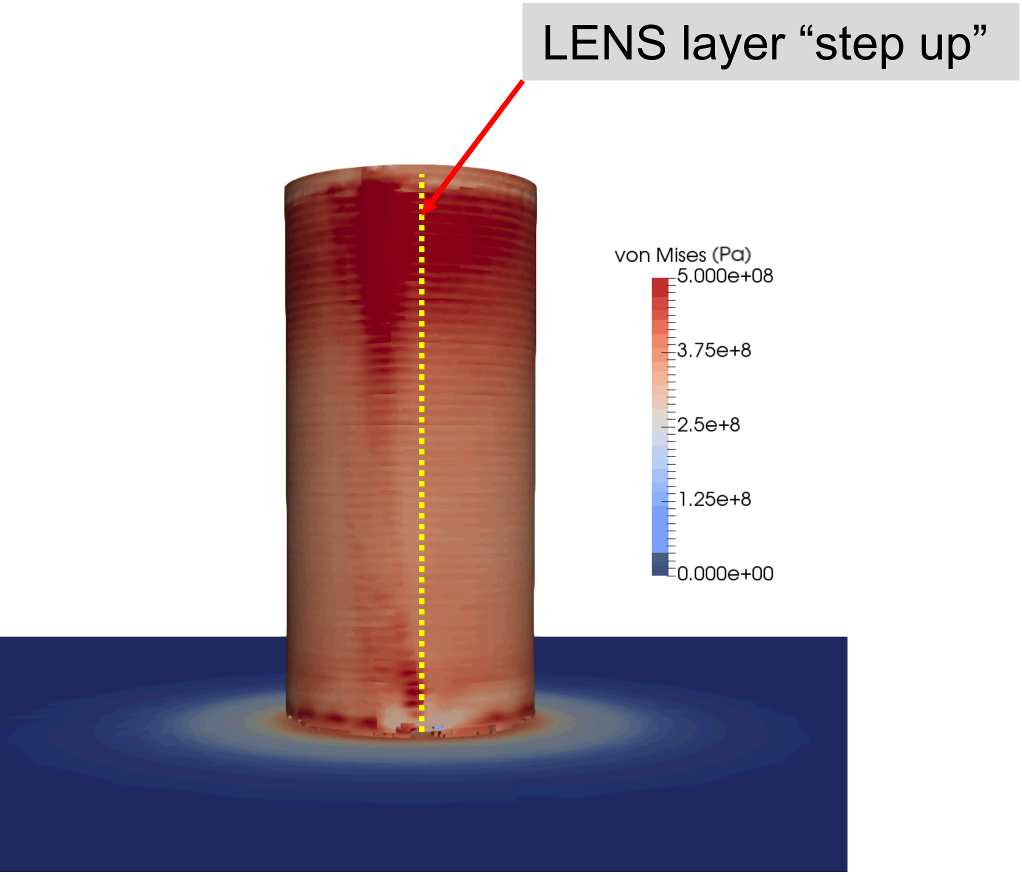

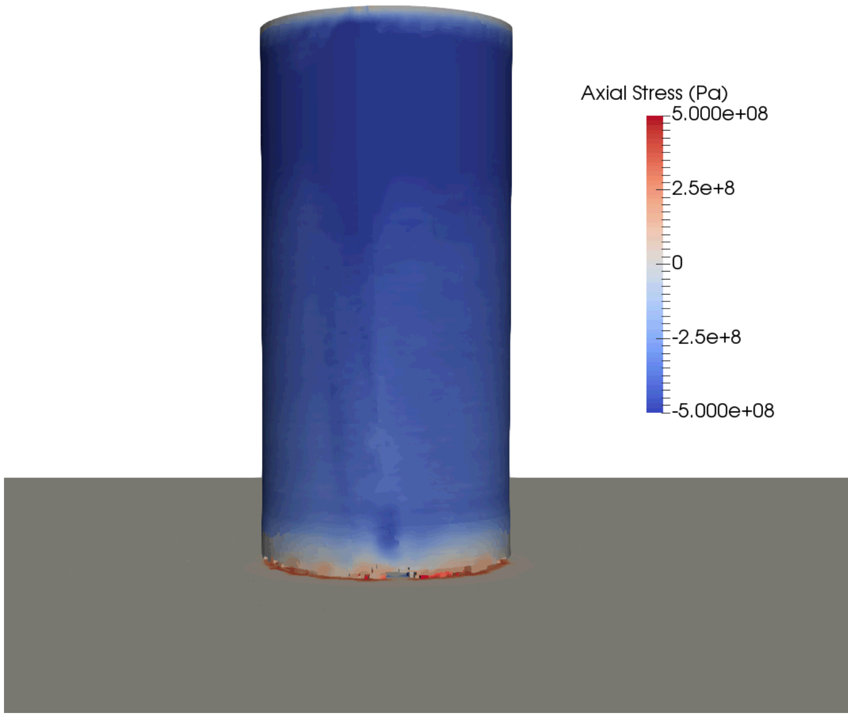

- Images taken after cool-down

Microstructure Prediction in SPPARKS

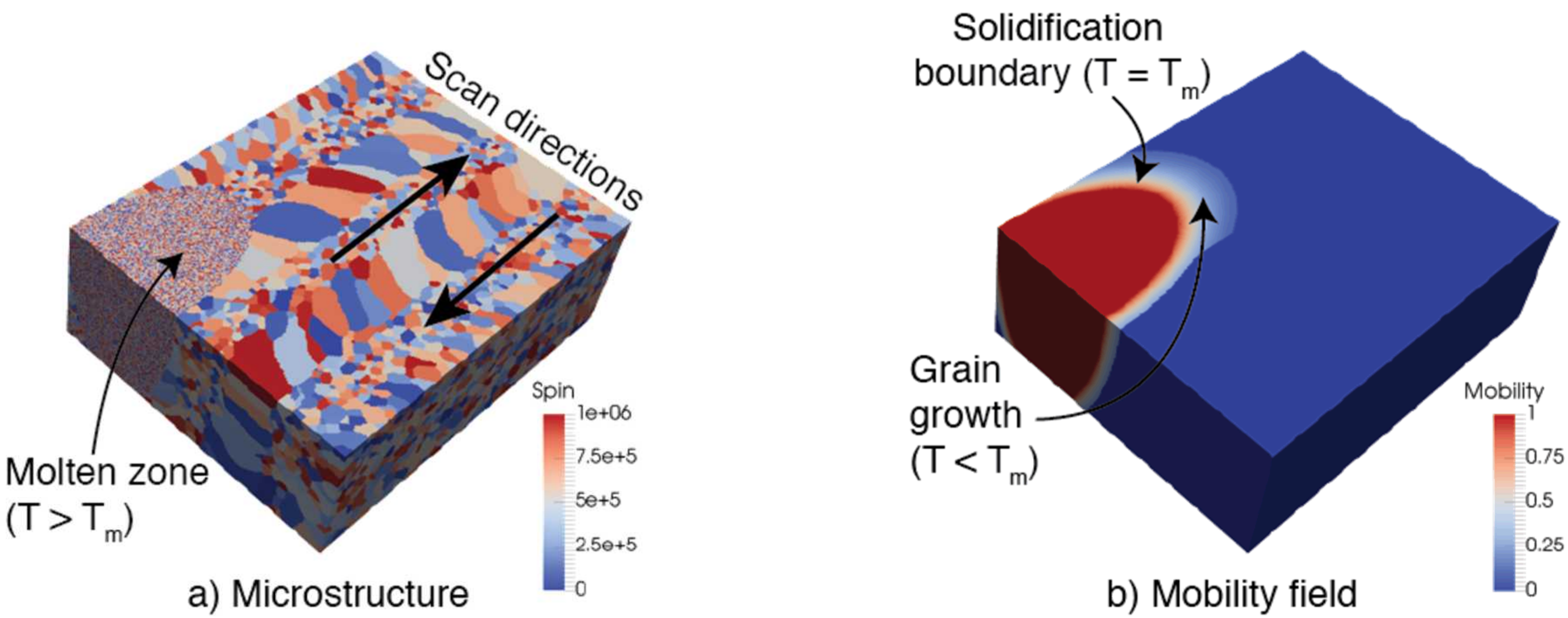

$$M(T) = M_o \exp\left(\frac{-Q}{RT}\right)$$

$$P = \begin{cases} M(T)\exp\left(\frac{-\Delta E}{k_B T_s}\right), & if\ \Delta E > 0 \\ M(T), & if\ \Delta E \leq 0 \end{cases}$$

- Aria temperature history is used as material state in SPPARKS
- Captures bulk heating effects on microstructure

Microstructure Demonstrates Equiaxed to Columnar Grain Transition

[redacted]

Equiaxed to Columnar Transition Observed in Literature

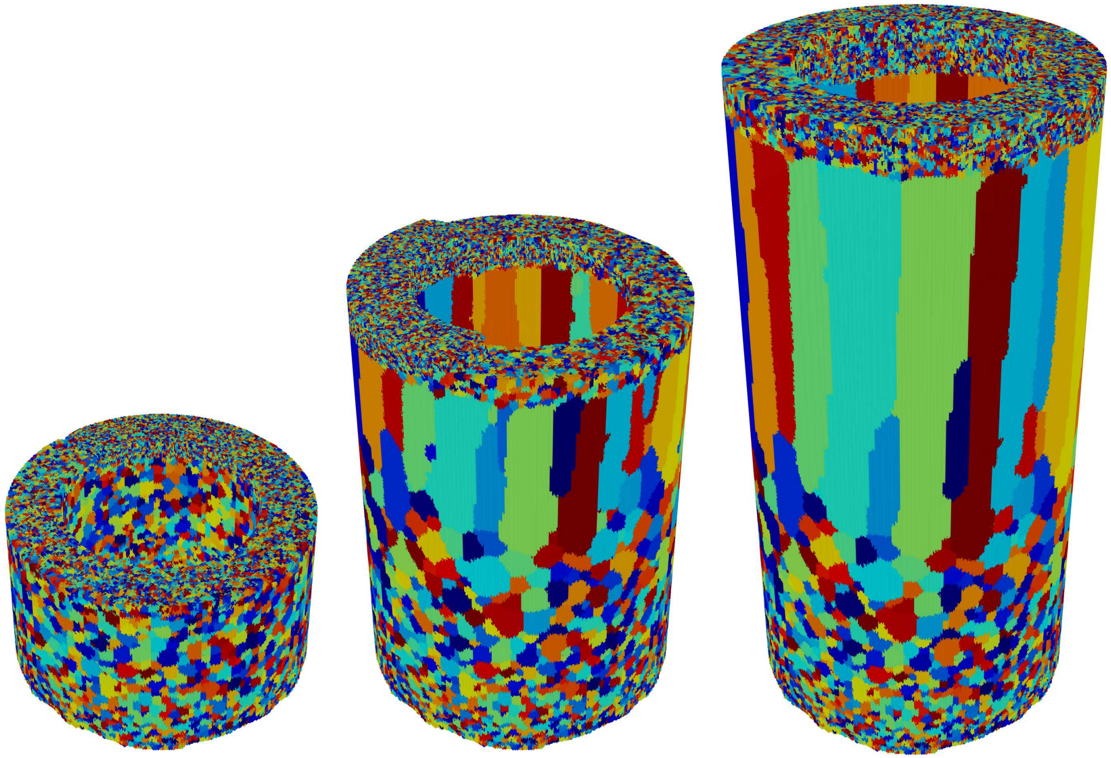

T=137 s   T=273 s   T=410 s

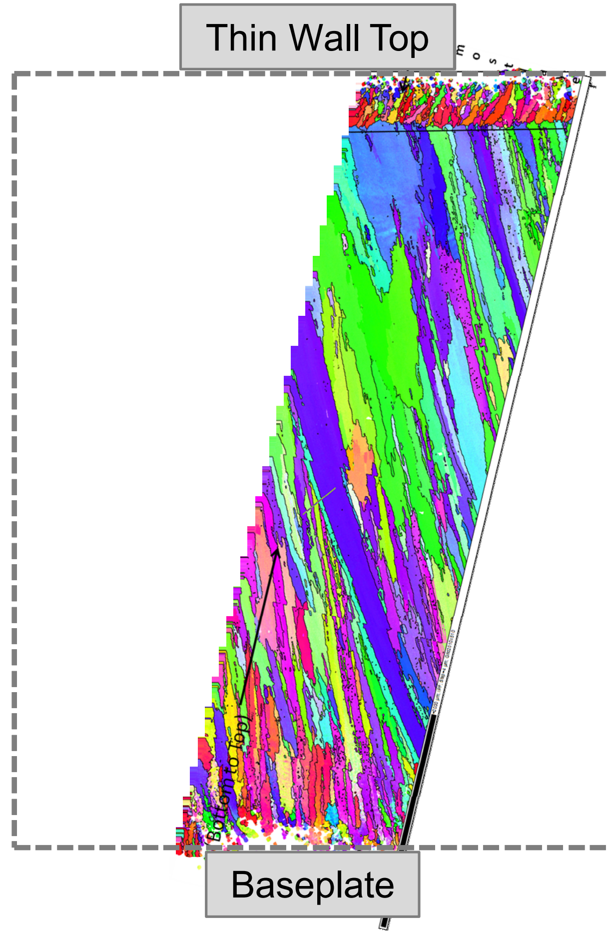

Thin wall IN718 LENS build at 900 W
Parimi *et al.* 2013

Effect of texture on homogenized elastic properties

(J. Bishop)

austenite grain (FCC)

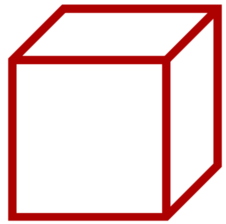

cubic symmetry

$$E = 93.8 \text{ GPa}$$
$$\nu = 0.402$$
$$G = 126 \text{ GPa}$$

$$G' \doteq \frac{E}{2(1+\nu)} = 33.4 \text{ GPa}$$

$$\frac{G}{G'} \approx 3.8$$ anisotropy ratio

no texture

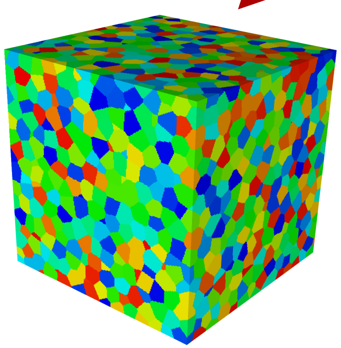

isotropic

$$E = 198 \text{ GPa}$$
$$\nu = 0.294$$
$$G = 76.5 \text{ GPa}$$

$$G = \frac{E}{2(1+\nu)}$$

ideal fiber-texture along [001]

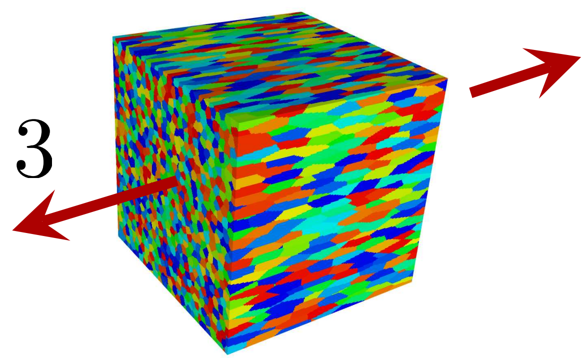

transversely isotropic

$$E_{11} = 143 \text{ GPa}$$
$$E_{22} = 143 \text{ GPa}$$
$$E_{33} = 90.9 \text{ GPa}$$
$$\nu_{12} = 0.114$$
$$\nu_{23} = 0.615$$
$$\nu_{13} = 0.615$$
$$G_{12} = 58 \text{ GPa}$$
$$G_{23} = 126 \text{ GPa}$$
$$G_{13} = 126 \text{ GPa}$$

Summary

- Presented activities and goals for powder bed fusion, thermal-mechanical processing and performance modeling
- Highlighted current capabilities we are leveraging for thermal-mechanical modeling of AM
- SNL is also focusing on impact of UQ, optimization, error estimation for AM